

1 **Title**

2

3 ***Development and validation of blood-based prognostic biomarkers for***
4 ***severity of COVID disease outcome using EpiSwitch 3D genomic***
5 ***regulatory immuno-genetic profiling.***

6

7 **Authors**

8 Ewan Hunter¹, Christina Koutsothanasi¹, Adam Wilson¹, Francisco C.
9 Santos¹, Matthew Salter¹, Jurjen W. Westra¹, Ryan Powell¹, Ann Dring¹,
10 Paulina Brajer¹, Benedict Egan¹, Matthew Parnall¹, Catriona Williams¹,
11 Aemilia Katzinski¹, Thomas Lavin¹, Aroul Ramadass¹, William Messer²,
12 Amanda Brunton², Zoe Lyski², Rama Vancheeswaran³, Andrew Barlow³,
13 Dmitri Pchejetski⁴, Peter A. Robbins^{5, 7}, Jane Mellor^{6, 7}, Alexandre
14 Akoulitchev¹

15

16 1 Oxford BioDynamics Plc, Oxford UK

17 2 Oregon Health & Science University, Portland, OR

18 3 West Hertfordshire NHS Trust, Watford, UK

19 4 Norwich Medical School, University of East Anglia

20 5 Department of Physiology, Anatomy and Genetics, University of Oxford,
21 Oxford, UK

22 6 Department of Biochemistry, University of Oxford, Oxford, UK

23 7 The Queen's College, University of Oxford, Oxford, UK

24

25 Address correspondence to: alexandre.akoulitchev@oxfordbiodynamics.com

26

27 Author e-mails:

28 Ewan Hunter: ewan.hunter@oxfordbiodynamics.com

29 Christina Koutsothanasi: christina.koutsothanasi@oxfordbiodynamics.com

30 Adam Wilson: adam.wilson@oxfordbiodynamics.com

31 Francisco Coroado Santos: francisco.santos@oxfordbiodynamics.com

32 Matthew Salter: matthew.salter@oxfordbiodynamics.com

33 Jurjen Westra: willem.westra@oxfordbiodynamics.com

34 Ryan Powell: ryan.powell@oxfordbiodynamics.com

35 Ann Dring: ann.dring@oxfordbiodynamics.com

36 Paulina Brajer: paulina.brajer@oxfordbiodynamics.com

37 Benedict Egan: benedict.egan@oxfordbiodynamics.com

38 Matthew Parnall: matthew.parnall@oxfordbiodynamics.com

39 Catriona Williams: catriona.williams@oxfordbiodynamics.com

40 Aemilia Katzinski: aemilia.katzinski@oxfordbiodynamics.com

41 Thomas Lavin: tomas.lavin@oxfordbiodynamics.com

42 William Messner: messner@ohsu.edu

43 Amanda Brunton: brunton@ohsu.edu

44 Zoe Lyski: lyski@ohsu.edu

45 Peter Robbins: peter.robbins@dpag.ox.ac.uk

46 Jane Mellor: jane.mellor@bioch.ox.ac.uk
47 Rama Vancheeswaran: rama.vancheeswaran @nhs.net
48 Andrew Barlow: a.barlow1@nhs.net
49 Dmitri Pchejetski: d.pshezhetskiy@uea.ac.uk
50 Alexandre Akoulitchev: alexandre.akoulitchev@oxfordbiodynamics.com
51

52 **Abstract**

53 The COVID-19 pandemic has raised several global public health challenges to
54 which the international medical community have responded. Diagnostic testing
55 and the development of vaccines against the SARS-CoV-2 virus have made
56 remarkable progress to date. As the population is now faced with the complex
57 lifestyle and medical decisions that come with living in a pandemic, a forward-
58 looking understanding of how a COVID-19 diagnosis may affect the health of
59 an individual represents a pressing need. Previously we used whole genome
60 microarray to identify 200 3D genomic marker leads that could predict mild or
61 severe COVID-19 disease outcomes from blood samples in a multinational
62 cohort of COVID-19 patients. Here, we focus on the development and validation
63 of a qPCR assay to accurately predict severe COVID-19 disease requiring
64 intensive care unit (ICU) support and/or mechanical ventilation. From 200
65 original biomarker leads we established a classification model containing six
66 markers. The markers were qualified and validated on 38 COVID-19 patients
67 from an independent cohort. Overall, the six-marker model obtained a positive
68 predictive value of 93% and balanced accuracy of 88% across 116 patients for
69 the prognosis of COVID-19 severity requiring ICU care/ventilation support. The
70 six-marker signature identifies individuals at the highest risk of developing
71 severe complications in COVID-19 with high predictive accuracy and can assist
72 in patient prognosis and clinical management decisions.

73

74

75 **Background**

76 The COVID-19 outbreak, which the World Health Organization (WHO) declared
77 a pandemic in March 2020, represents one of the greatest global health crises
78 the world has faced in recent history [1]. In addition to the estimated 130+
79 million people that have been infected with the SARS-CoV-2 virus to date and
80 the more than 3 million deaths attributed to COVID-19 related causes; the
81 pandemic has placed tremendous strain on healthcare systems, caused
82 devastating mental health crises, and tested global economic resiliency [2, 3].
83 In response to the COVID-19 crisis, the global research and medical
84 communities responded quickly with the rapid development and deployment of
85 diagnostic tests to identify individuals who are currently infected or have
86 previously been infected with the SARS-CoV-2 virus. As of March 2021, over
87 250 different rapid antigen or molecular tests to detect SARS-CoV-2 have
88 received Emergency Use Authorization by the US FDA alone [4, 5]. For several
89 reasons, including the early immediate unmet need to identify SARS-CoV-2
90 positive individuals and the lack of availability of real-world data on how different
91 individuals respond to the virus, research on features that are predictive for
92 different manifestations of COVID-19 have lagged behind the development of
93 diagnostic testing. The few predictive measures that have been assessed suffer
94 from low certainty, high bias, and insufficient predictive accuracy [6]. As
95 clinicians have gained experience in treating COVID-19 patients, one of the
96 more striking observations has been the wide range of clinical manifestations
97 of the disease in different individuals; many of which could not be predicted by

98 basic clinical parameters such as age, gender, or pre-existing conditions/co-
99 morbidities alone [7–9]. It is now clear that the variability in host response,
100 rather than viral genetics or load, is the primary determinant of the wide range
101 of observed disease manifestations.

102

103 While diagnostic testing is now routine, there remains a pressing need to
104 develop molecular readouts that can reveal individual susceptibility to
105 developing severe COVID-19 symptoms in response to the SARS-CoV-2 virus
106 with high predictive accuracy to support clinical decision making and patient
107 management [10]. Specifically, there is a need to develop accurate, non-
108 invasive tests to identify prognostic profiles for clinical cases where patients
109 develop hyperinflammation, do not respond to the standard of care, and
110 progress to needing ICU-level support and/or mechanical ventilation in
111 accordance with the WHO severity definitions [10]. Individualized knowledge
112 of disease severity risk can help people take appropriate precautions in their
113 daily lives, understand how a COVID-19 diagnosis may impact a pre-existing
114 medical condition, anticipate and plan for medical treatment if they become
115 infected, and decrease their personal risk of contracting severe symptoms by
116 managing risk factors. All of these are critical tools for managing the global
117 health crisis, even in the face of the recent development of COVID-19 vaccines.
118 The first vaccines against the SARS-CoV-2 virus became available in the late
119 2020 and represented a major step forward in containing the spread of the virus
120 and its myriad social tolls [11–13]. However, several factors may limit the
121 effectiveness of universal vaccination: 1) vaccine shortages and limited national
122 vaccination rates 2) contraindications in certain patient populations (e.g.

123 children under 18, individuals who have certain health conditions, such as
124 recent infections and anaphylaxis) 3) individual decisions to forego vaccination
125 and 4) reductions in vaccine efficacy in newly emerging SARS-CoV-2 variants
126 as demonstrated recently in a Chilean population with persistently high infection
127 rates despite the availability of the CoronaVac vaccine and >40% national
128 vaccination rates [14]. As such, the ability for individuals and their physicians
129 to understand the risk of developing severe symptoms if infected with the
130 SARS-CoV-2 virus remains a critical unmet healthcare need.

131

132 Recently, we reported on the use of *EpiSwitch*®, a chromosome conformation
133 capture (3C) methodology that has been reduced to practice for the discovery
134 of blood-based 3D genomic biomarkers and patient stratification in a variety of
135 immune-related diseases, to identify prognostic profiles that could serve as a
136 potential blood-based molecular classifier for the prediction of COVID-19
137 disease severity [15–22]. Specifically, we used *EpiSwitch* Explorer 3D whole
138 genome arrays to identify changes at immune-related loci in blood samples
139 from a multi-national cohort of COVID-19 patients. We identified 200 array-
140 based 3D genomic marker leads that could differentially predict mild or severe
141 COVID-19 disease severity, with a high degree of sensitivity and specificity.
142 The proteins encoded at the locations of the 3D genomic marker leads were
143 involved in biological pathways with direct relevance to immune system function
144 including T-cell signalling, macrophage-stimulating protein (MSP)-RON
145 signalling, and calcium signalling [15]. The aim of this study was an extension
146 of our previous work, using the established *EpiSwitch* platform to translate the
147 array-derived 3D genomic biomarkers into a qPCR-based testing format, refine

148 and reduce the biomarker panel, build a classification model and perform
149 validation on independent COVID-19 patient cohorts. Here we report on the
150 development of a 3D genomic biomarker panel with clinical utility in predicting
151 disease severity in COVID-19.

152

153 **Materials and Methods**

154 *Patient characteristics*

155 Clinical whole blood samples from consented patients were supplied from Boca
156 Biolistics LLC (FL, USA) and Reprocell USA Inc. (MD, USA). A total of 116
157 patients from three sample cohorts were used in this study, comprising a
158 multinational set of COVID-19 cases from the United States, Peru, and the
159 Dominican Republic. Patient annotations are listed in (**Supplemental Tables**
160 **1,2**). In line with WHO guidelines, the patient annotations provided were used
161 to classify the severe outcome group on the basis of a confirmed admission to
162 the Intensive Care Unit (ICU) and/or advanced clinical interventions such as
163 mechanical ventilation [10]. Patients that required a lower level of clinical care,
164 such as administration of supplemental oxygen only, were classified as the mild
165 outcome group. All samples were collected within 72 hours of a patient being
166 admitted to a hospital for treatment of a PCR-confirmed COVID infection. The
167 age of the patients ranged from 28 to 92, with median of 64.5 years
168 (**Supplemental Tables 1, 2**).

169

170 *Preparation of 3D genomic templates*

171 *EpiSwitch*[®] 3C libraries, with chromosome conformation analytes converted to
172 sequence based tags, were prepared from frozen whole blood samples using

173 *EpiSwitch*[®] protocols following the manufacturer's instructions (Oxford
174 BioDynamics Plc) [15]. All samples were processed under biological
175 containment level CL2+. Initial sample processing was performed manually in
176 a Category 3 microbial safety cabinet with the remainder performed on the
177 Freedom EVO 200 robotic platform (Tecan Group Ltd). Briefly, 50 μ L of whole
178 blood sample was diluted and fixed with a formaldehyde containing *EpiSwitch*
179 buffer. Density cushion centrifugation was used to purify intact nuclei. Following
180 a short detergent-based step to permeabilise the nuclei, restriction enzyme
181 digestion and proximity ligation were used to generate the 3C libraries.
182 Samples were centrifuged to pellet the intact nuclei before purification with an
183 adapted protocol from the QIAmp DNA FFPE Tissue kit (Qiagen) Eluting in 1x
184 TE buffer pH7.5. 3C libraries were quantified using the Quant-iT[™] Picogreen
185 dsDNA Assay kit (Invitrogen) and normalised to 5 ng/ μ l prior to interrogation by
186 PCR.

187

188 *Translation of array-based 3D genomic markers to PCR readouts*

189 The top array-derived markers identified in our previous study were
190 interrogated using OBD's proprietary primer design software package to
191 identify genomic positions suitable for a hydrolysis probe based real time PCR
192 (RT-PCR) assay [15]. Briefly, the top array-derived markers associated with
193 prognostic potential to differentiate between mild and severe COVID disease
194 outcomes were filtered on fold change and adjusted p value. PCR primer
195 probes were ordered from Eurofins genomics as salt-free primers. The probes
196 were designed with a 5' FAM fluorophore, 3' IABkFQ quencher and an
197 additional internal ZEN quencher and ordered from iDT (integrated DNA

198 Technologies) [23]. Each assay was optimised using a temperature gradient
199 PCR with an annealing temperature range from 58-68° C. Individual PCR
200 assays were tested across the temperature gradient alongside negative
201 controls including soluble and unstructured commercial TaqMan human
202 genomic DNA control (Life Technologies) and used a TE buffer only negative
203 control. Assay performance was assessed based on Cq values and reliability
204 of detection and efficiency based on the slope of the individual amplification
205 curves. Assays that passed the quality criteria and presented with reliable
206 detection differences between the pooled samples associated with Severe and
207 Mild COVID disease outcomes were used to screen individual patient samples.

208

209 *EpiSwitch PCR*

210 Each patient sample was interrogated using RT-PCR in triplicate. Each reaction
211 consisted of 50 ng of EpiSwitch library template, 250 mM of each of the primers,
212 200 mM of the hydrolysis probe and a final 1X Kapa Probe Force Universal
213 (Roche) concentration in a final 25 µl volume. The PCR cycling and data
214 collection was performed using a CFX96 Touch Real-Time PCR detection
215 system (Bio-Rad). The annealing temperature of each assay was changed to
216 the optimum temperature identified in the temperature gradients performed
217 during translation for each assay. Otherwise, the same cycling conditions were
218 used: 98°C for 3 minutes followed by 45 cycles of 95°C for 10 seconds and 20
219 seconds at the identified optimum annealing temperature. The individual well
220 Cq values were exported from the CFX manager software after baseline and
221 threshold value checks. All Cq values obtained for individual samples and
222 markers are available online

223 [\[https://github.com/oxfordBiodynamics/medrxiv/tree/main/CST%20publication\]](https://github.com/oxfordBiodynamics/medrxiv/tree/main/CST%20publication)

224 . A total of 21 3D genomic markers that passed the translation phase were
225 screened on 78 individual samples from the Training cohort. A marker reduction
226 step based on statistical criteria were used to identify the top six discriminating
227 markers which were used to screen the remaining set of 38 samples in the Test
228 cohort.

229

230 *Genomic mapping*

231 The 21 3D genomic markers from the statistically filtered list with the greatest
232 and lowest abundance scores were selected for genome mapping. Mapping
233 was carried out using Bedtools *closest* function for the 3 closest protein coding
234 loci (Gencode v33). All markers were visualized using the *EpiSwitch* Data
235 Portal.

236

237 *Statistical analysis*

238 The 21 markers screened on 78 individual patient samples were subject to
239 permuted logistic modelling with bootstrapping for 500 data splits and non-
240 parametric Rank Product analysis (EpiSwitch® RankProd R library). Two
241 machine learning procedures (eXtreme Gradient Boosting: XGBoost and
242 CatBoost) were used to further reduce the feature pool and identify the most
243 predictive/prognostic, 3D genomic markers. The resulting markers were then
244 used to build the final classifying models using CatBoost and XGBoost. All
245 analysis was performed using R statistical language with Caret, XGBoost,
246 SHAPforxgboost and CatBoost libraries.

247

248 *Biological network/pathway analysis*

249 Pathway enrichment analysis was performed using the Reactome Pathway
250 Browser [24]. Protein interaction networks were generated using the Search
251 Tool for the Retrieval of Interacting proteins (STRING) database [24, 25].

252

253 **Results**

254 **Identification of the top prognostic 3D genomic markers for severe** 255 **COVID-19 disease outcomes**

256 In this study we employed a sequential stepwise strategy to identify a minimal
257 set of biomarkers that were predictive of COVID-19 disease severity (**Figure**
258 **1**). Starting with an initial set of 200 array-derived 3D genomic marker leads
259 identified in our previously published work, here we used independent sets of
260 116 whole blood samples collected at the time of confirmed COVID-19 infection
261 from patients in the United States, Peru, and the Dominican Republic to refine
262 and test the prognostic 3D genomic biomarker panel. Whole blood samples
263 were procured for a Training cohort used to build and refine the classifier model,
264 and Test cohort to assess the predictive performance of the model. Clinical
265 characteristics of the patients are shown in **Table 1 and Supplemental Tables**
266 **1, 2**. To translate the *EpiSwitch* Explorer Array markers to a PCR-detectable
267 assay, primers to detect individual 3D genomic markers were generated and
268 validated (Materials & Methods). Using a 78 sample Training set of COVID-19
269 patient whole blood samples, feature reduction using machine learning
270 methods on the initial pool of 200 3D genomic biomarkers identified 21 markers
271 with predictive power to differentiate between COVID-19 patients that required
272 a high degree of medical disease management (e.g. admission to the intensive

273 care unit (ICU), mechanical ventilation) and those that were hospitalized but
274 required less interventional care and support (Supplemental **Table 1, for Cq**
275 **data see online link –**
276 <https://github.com/oxfordBiodynamics/medrxiv/tree/main/CST%20publication>).

277 We found the top 21 markers to be non-randomly distributed throughout the
278 human genome, with notable enrichment on larger chromosomes and a
279 hotspots on chromosome 11 (**Figure 2A**). Four out of the 21 markers
280 associated with ICU outcomes occurred within an approximately 265 kb region
281 on the p-arm of chromosome 11 containing the switching B cell complex subunit
282 SWAP70 (SWAP70) locus (**Figure 2B**). While some of the 3D genomic markers
283 were localized within protein coding regions of single genes (**Figure 2C**), other
284 markers spanned the protein coding regions of multiple genes (**Figure 2B**).
285 Pathway enrichment for genes contained within the 21 3D genomic markers
286 revealed the top two pathways to be related to downstream signalling mediated
287 by B-cell receptor activation (**Table 3**). Importantly, genomic loci encoding
288 proteins involved in hemostasis/clotting were also enriched (**Figure 3, Table**
289 **3**). The 21 3D genomic markers were further refined to a set of 6 markers (**Table**
290 **4**) with predictive ability for COVID severity and applied to an independent Test
291 cohort (Supplemental **Table 2**).

292

293 **Testing of the prognostic 3D genomic biomarker panel for severe COVID-** 294 **19 disease outcomes on independent patient cohorts.**

295 To assess the predictive power of the model, the 6-marker 3D genomic panel
296 was validated on an independent (samples that were not used to build and
297 refine the model) Test cohort (**Figure 4, Supplemental Table 2**). Samples were

298 collected upon admission to COVID hospital wards in Peru, the USA, and the
299 Dominican Republic and shipped to OBD's processing facility in Oxford, UK.
300 The *EpiSwitch* platform read outs for the six-marker classifier model were
301 uploaded to the *EpiSwitch* Analytical Portal for analysis. Classifier calls for high-
302 risk COVID-19 disease outcomes are shown in **Table 5**. Clinical outcomes for
303 the Test cohort included 10 mild cases or 28 severe cases requiring ventilation
304 and/or ICU support. *EpiSwitch* prognostic calls based on the 6-marker model
305 demonstrated performance of 90.9% positive predictive value for high-risk
306 disease outcomes in the Test cohort (**Figure 4A**). Interestingly, two of the mild
307 case patients (COVID 0696 and 0213) (**Table 5**), identified as high risk by the
308 *EpiSwitch* test subsequently died in the hospital within 28 days of admission.
309 This suggests an early, pre-symptomatic detection of a hyperinflammatory state
310 leading to fatal outcomes and is being investigated further. Across all 116
311 patients used in this study, the test demonstrated positive predictive value for
312 high-risk disease outcomes of 92.9 with, 88% sensitivity, 87% specificity, and
313 a balanced accuracy of 87.9% (**Table 4B and Supplementary Table 3**).

314

315

316

317

318

319

320

321

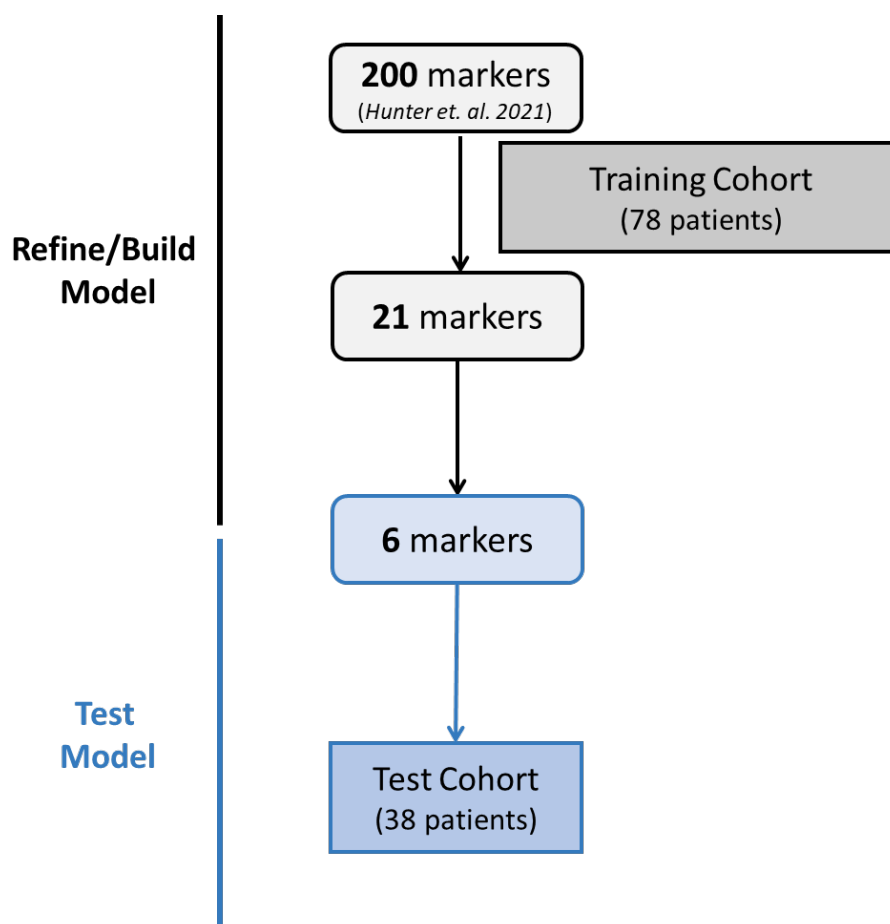
322

323

324

325 **Figures & Tables**

326



327

328 **Figure 1. Simplified workflow used to develop and test the prognostic 3D**

329 **genomic classifier model for prediction of COVID-19 disease severity.**

330 Starting from a list of 200 3D genomic markers identified by Hunter et al. 2021,

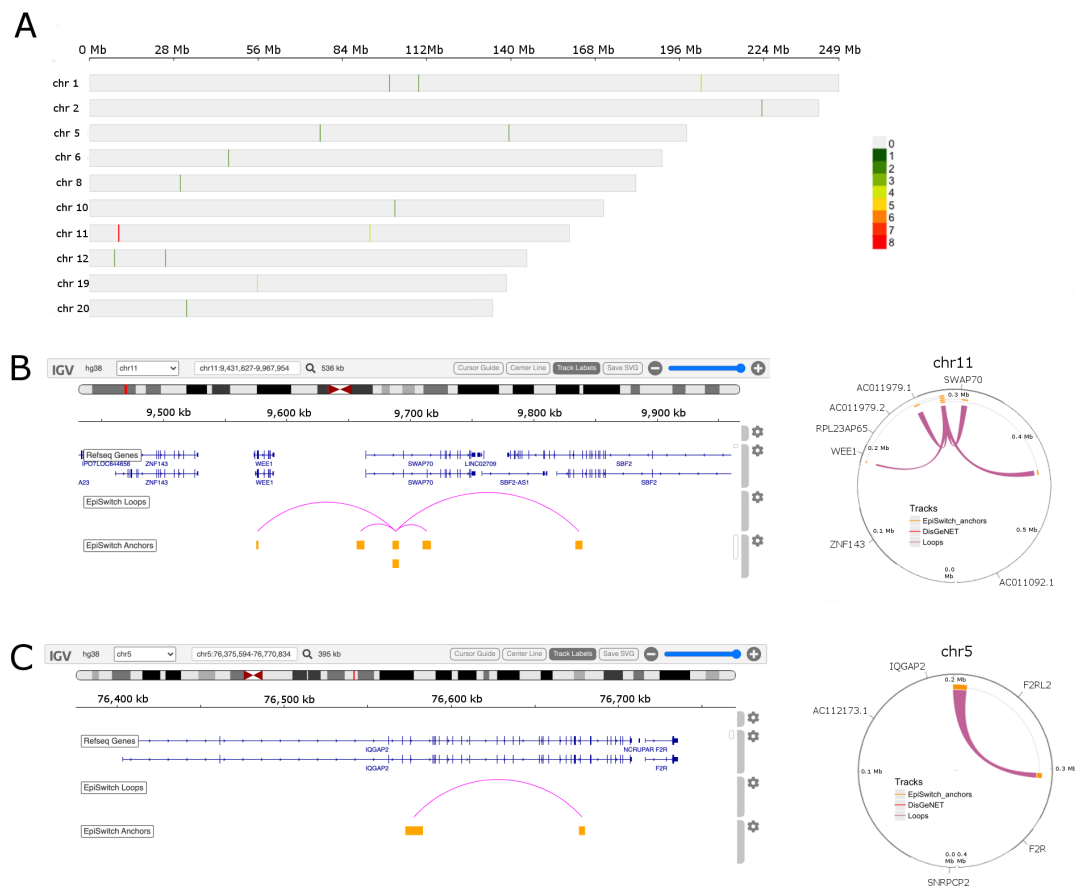
331 we used a sequential, stepwise approach employing a 78-patient Training

332 cohort to refine the marker set and build a predictive classifier model containing

333 six 3D genomic markers. The 6-marker model/assay was tested on an

334 independent Test cohort of 38 COVID-19 patient blood samples.

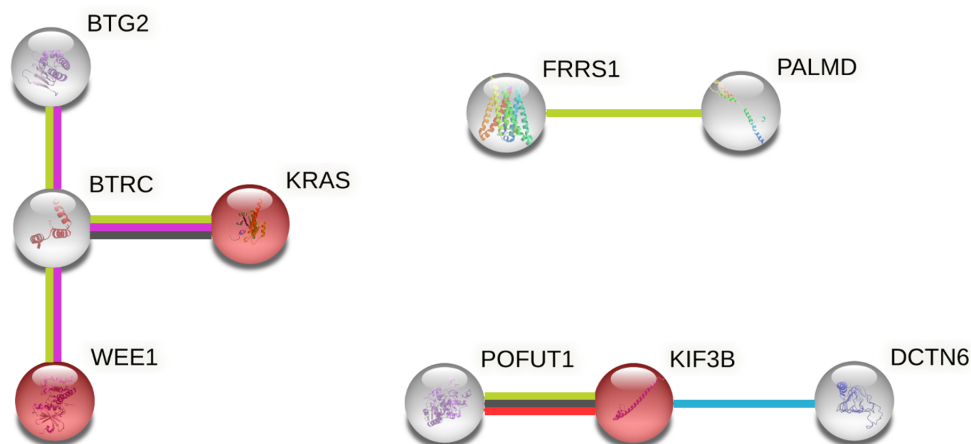
335



336

337 **Figure 2. Genomic detail view of top prognostic 3D genomic biomarkers.**

338 **A.** Genomic locations and distribution of the top 21 3D genomic biomarkers for
339 Hospitalized and ICU clinical outcomes. Individual human chromosomes where
340 the top 21 markers were found are shown on the y-axis. The heatmap shows
341 the number of markers within a 0.3Mb genomic window with green representing
342 a low density of markers and red indicating a high density of markers. A region
343 on chromosome 11 shows a high density of markers associated with ICU
344 outcomes. **B.** Linear and circos plot views of a ~500 kb region of chromosome
345 11 containing the SWAP70 locus showing the genomic location for four
346 markers. **C.** Linear and circos views of a ~400 kb region of chromosome 5
347 containing the IQGAP2 and F2RL2 loci showing the genomic location for one
348 of the markers in the final 6-marker set.



349

350 **Figure 3. STRING network for top 3D genomic markers.** Protein-protein
 351 interaction network for proteins encoded by genes spanning the top 21 3D
 352 genomic marker set. Edges are colored by protein-protein association type
 353 (blue = known interactions from curated databases, magenta = known
 354 interactions from experiments, light green = interactions derived from literature
 355 text mining, orange = gene fusions, black = association by co-expression).
 356 Nodes highlighted in red are associated with the Reactome ‘Hemostasis’
 357 pathway (HSA-109582).

358

A	Severe Outcome				Total
	Test	Present	n	Absent	
Yes	True Positive	20	False Positive	2	22
No	False Negative	8	True Negative	8	16
Total		28		10	

B	Severe Outcome				Total
	Test	Present	n	Absent	
Yes	True Positive	66	False Positive	5	71
No	False Negative	9	True Negative	36	45
Total		75		41	

Results Statistic	Value	95% CI
Sensitivity	71.43%	51.33% to 86.78%
Specificity	80.00%	44.39% to 97.48%
Positive Likelihood Ratio	3.57	1.01 to 12.61
Negative Likelihood Ratio	0.36	0.18 to 0.69
Disease prevalence*	73.68%	56.90% to 86.60%
Positive Predictive Value*	90.91%	73.90% to 97.25%
Negative Predictive Value*	50.00%	34.02% to 65.98%
Accuracy*	73.68%	56.90% to 86.60%

Results Statistic	Value	95% CI
Sensitivity	88.00%	78.44% to 94.36%
Specificity	87.80%	73.80% to 95.92%
Positive Likelihood Ratio	7.22	3.16 to 16.48
Negative Likelihood Ratio	0.14	0.07 to 0.25
Disease prevalence*	64.66%	55.24% to 73.31%
Positive Predictive Value*	92.96%	85.25% to 96.79%
Negative Predictive Value*	80.00%	68.20% to 88.18%
Accuracy*	87.93%	80.58% to 93.24%

359

360 **Figure 4. Performance of the prognostic biomarker classifier for calling**
 361 **high risk of severe disease outcome on COVID-19 patient cohorts. (A)**

362 Confusion matrix and test performance statistics for the 6-marker classifier on
 363 the 38 patients of the Test cohort (B) and the 116 patients in the combined
 364 Training and Test cohorts. Note: (*) These values are dependent on disease
 365 prevalence

366

367 **Table 1. Summary of clinical characteristics by cohort for COVID-19**
 368 **patient samples used in this study.** Clinical features of the 116 COVID-19
 369 patient samples used in this study by cohort. SD: Standard deviation; PEC: pre-
 370 existing condition; Hosp.: Hospitalized; ICU: Intensive Care Unit; SO: Received
 371 supplemental oxygen; Vent.: Received mechanical ventilation.

Cohort	N	% male	% female	Age (mean)	Age (SD^a)	% w/PEC^b	% Hosp.^c	% ICU^d	% SO^e	% Vent.^f
Training	78	64	36	64.8	14.5	76	46	54	37	60
Test	38	79	21	65.1	16.2	90	53	47	29	74

372 ^a Standard deviation

373 ^b pre-existing condition

374 ^c Hospitalized

375 ^d Intensive Care Unit

376 ^e Received supplemental oxygen

377 ^f Received mechanical ventilation

378

379 **Table 2. List of the top 21 3D genomic markers for prediction of COVID-19**
 380 **disease severity.** List of the top 21 markers with predictive ability for COVID-
 381 19 severity. Markers are listed by the OBD internal ID. The six markers in the
 382 final 3D genomic panel are outlined in red. The closest protein-coding genes
 383 near the 3D genomic markers are also listed (Closest Genes).

Marker^a	Closest Genes^b
hg38_10_101411215_101490136_RF	BTRC,DPCD,POLL
hg38_11_9577172_9685884_FR	AC011979.1,AC011979.2,RPL23AP65,SWAP70,WEE1
hg38_20_32238035_32290178_FF	KIF3B,PLAGL2,POFUT1
hg38_11_9685855_9716901_RF	AC011979.1,AC011979.2,SWAP70
hg38_1_109341941_109359750_RR	MYBPHL,PSMA5,SORT1
hg38_11_9663012_9685884_FR	AC011979.1,AC011979.2,SWAP70
hg38_5_139331499_139356679_FF	MATR3,PAIP2,SLC23A1

hg38_2_223395100_223450604_FF	AP1S3,HIGD1AP4,KCNE4,SCG2
hg38_1_99670351_99714401_FF	AGL,FRRS1,HMGB3P10,PALMD
hg38_8_30132538_30177089_RR	DCTN6,LEPROTL1,MBOAT4
hg38_12_8219312_8342000_RR	AC092745.2,AC092745.3,ALG1L10P,CLEC4A,ENPP7P5, FAM86FP,FAM90A1
hg38_11_9685855_9839717_RF	AC011979.1,SBF2,SWAP70
hg38_19_55694909_55778461_RF	AC008749.1,AC010525.2,EPN1,NLRP9,RFPL4A,RFPL4A L1,RFPL4AP1
hg38_6_46139224_46175482_FF	ACTG1P9,ENPP4,ENPP5
hg38_12_25206967_25256704_FR	CASC1,ETFRF1,KRAS
hg38_11_93198707_93237221_RR	SLC36A4;MTNR1B;DEUP1
hg38_5_76572659_76680168_RF	F2R,F2RL2,IQGAP2
hg38_1_203182882_203350382_FR	BTG2,CHI3L1,CHIT1,FMOD,NPM1P40
hg38_19_55711884_55778461_RF	NLRP9,RFPL4A,RFPL4AL1,RFPL4AP1
hg38_1_203182882_203368482_FF	AL359837.1,BTG2,CHI3L1,CHIT1,FMOD,NPM1P40
hg38_11_93057516_93237221_RR	SLC36A4;MTNR1B;DEUP1

384

Pathway identifier ^a	Pathway name ^b	#Entities found ^c	#Entities total ^d	Entities ratio ^e	Entities pValue ^f	Entities FDR ^g	#Reactions found ^h	#Reactions total ⁱ	Reactions ratio ^j	Species name ^k
R-HSA-1168372	Downstream signaling events of B Cell Receptor (BCR)	3	91	0.006266354	8.80E-04	0.008475369	3	15	0.001117235	Homo sapiens
R-HSA-983705	Signaling by the B Cell Receptor (BCR)	3	189	0.013014736	0.006883631	0.019502853	3	44	0.003277223	Homo sapiens
R-HSA-5621481	C-type lectin receptors (CLRs)	3	203	0.013978791	0.008365905	0.019502853	7	68	0.0050648	Homo sapiens
R-HSA-69275	G2/M Transition	3	212	0.01459854	0.009410889	0.019502853	8	78	0.005809623	Homo sapiens
R-HSA-453274	Mitotic G2-G2/M phases	3	214	0.014736262	0.009653045	0.019502853	8	80	0.005958588	Homo sapiens
R-HSA-2454202	Fc epsilon receptor (FCERI) signaling	3	235	0.016182344	0.012417469	0.024834939	2	63	0.004692388	Homo sapiens
R-HSA-416476	G alpha (q) signalling events	3	283	0.019487674	0.020298035	0.040596071	4	35	0.002606882	Homo sapiens
R-HSA-109582	Hemostasis	5	801	0.055157692	0.022922661	0.045845322	13	334	0.024877104	Homo sapiens
R-HSA-8856688	Golgi-to-ER retrograde transport	2	148	0.010191434	0.037413554	0.069833207	4	18	0.001340682	Homo sapiens
R-HSA-2132295	MHC class II antigen presentation	2	148	0.010191434	0.037413554	0.069833207	1	26	0.001936541	Homo sapiens
R-HSA-199991	Membrane Trafficking	4	665	0.045792591	0.046627545	0.069833207	12	219	0.016311634	Homo sapiens
R-HSA-168249	Innate Immune System	6	1333	0.091791764	0.052086077	0.069833207	14	708	0.052733502	Homo sapiens
R-HSA-1280218	Adaptive Immune System	5	1004	0.069136483	0.052885643	0.069833207	9	264	0.01966334	Homo sapiens
R-HSA-9013149	RAC1 GTPase cycle	2	191	0.013152458	0.059025208	0.069833207	2	6	4.47E-04	Homo sapiens
R-HSA-983231	Factors involved in megakaryocyte development and platelet production	2	194	0.013359041	0.060664833	0.069833207	5	43	0.003202741	Homo sapiens
R-HSA-6811442	Intra-Golgi and retrograde Golgi-to-ER traffic	2	218	0.015011706	0.074331183	0.074331183	4	48	0.003575153	Homo sapiens
R-HSA-6798695	Neutrophil degranulation	3	480	0.033053298	0.075629054	0.075629054	4	10	7.45E-04	Homo sapiens
R-HSA-168256	Immune System	9	2681	0.184616444	0.086870431	0.086870431	29	1621	0.120735886	Homo sapiens
R-HSA-5653656	Vesicle-mediated transport	4	824	0.056741496	0.087750436	0.087750436	12	252	0.018769552	Homo sapiens
R-HSA-71240	Tryptophan catabolism	1	48	0.00330533	0.094550828	0.094550828	1	16	0.001191718	Homo sapiens

385 ^a The Reactome's Pathway Identifier.

386 ^b The Reactome's Pathway Name.

387 ^c The number of curated molecules of the type selected with Results Type that
 388 are common between the submitted data set and the pathway named in column
 389 1.

390 ^d The total number of curated molecules of the type selected with Results Type
 391 within the pathway named in column 1.

392 ^e The proportion of Reactome pathway molecules represented by this pathway.

393 Calculated as the ratio of entities from this pathway that are molecules of the

394 type selected with Results Type Vs.

395 ^f The result of the statistical test for over-representation, for molecules of the

396 results type selected.

397 ^g False discovery rate. Corrected over-representation probability.

398 ^h The number of reactions in the pathway that are represented by at least one

399 molecule in the submitted data set, for the molecule type selected with Results

400 Type.

401 ⁱ The number of reactions in the pathway that contain molecules of the type

402 selected with Results Type.

403 ^j The proportion of Reactome reactions represented by this pathway.

404 Calculated as the ratio of reactions from this pathway that contain molecules of

405 the type selected with Results Type Vs. all Reactome reactions that contain

406 molecules of the type selected with Results Type.

407 ^k The Species name

408

409 **Table 4. List of the top 6 3D genomic markers for prediction of COVID-19**

410 **disease severity.** List of the 6 markers that comprise the predictive COVID-

411 19 severity biomarker panel. Markers are listed by the OBD internal ID. The

412 closest protein-coding genes near the 3D genomic markers are also listed in

413 the 'Closest Genes' column.

Marker ^a	Closest Genes ^b
hg38_1_109341941_109359750_RR	MYBPHL,PSMA5,SORT1
hg38_5_76572659_76680168_RF	F2R,F2RL2,IQGAP2
hg38_2_223395100_223450604_FF	AP1S3,HIGD1AP4,KCNE4,SCG2
hg38_6_46139224_46175482_FF	ACTG1P9,ENPP4,ENPP5
hg38_8_30132538_30177089_RR	DCTN6,LEPROTL1,MBOAT4

hg38_19_55694909_55778461_RF

AC008749.1,AC010525.2,EPN1,NLRP9,RFPL4A,RFPL4AL1,RFPL4AP1

414 ^a **The marker's ID**

415 ^b **The genes around the genomic loci of the marker**

416

417

418 **Table 5. Prognostic calls for high-risk of severe outcome with the 6-**

419 **marker *EpiSwitch* classifier model.** Prognostic calls of average and high risk

420 for the 38 patients against disclosed attributes of severity: ventilation and /or

421 ICU support

Cohort	SampleID	COVID Severity		EpiSwitch Prognostic Call for High-Risk		Final Call
		Ventilation	ICU ^a	No	Yes	
Test	COVID0732	No	No	0.624535561	0.3754644	No
Test	COVID0129	No	No	0.989352465	0.0106475	No
Test	COVID0636	No	No	0.810631394	0.1893686	No
Test	COVID0189	No	No	0.96364671	0.0363533	No
Test	COVID0708	No	No	0.918016613	0.0819834	No
Test	COVID0117	No	No	0.760194659	0.2398053	No
Test	COVID0207	No	No	0.740656555	0.2593434	No
Test	COVID0380	No	No	0.990677834	0.0093222	No
Test	COVID0696	No	No	0.020404769	0.9795952	Yes*
Test	COVID0213	No	No	0.04568797	0.954312	Yes*
Test	COVID0606	Yes	No	0.809160769	0.1908392	No
Test	COVID0648	Yes	No	0.987436414	0.0125636	No
Test	COVID0642	Yes	No	0.665544152	0.3344558	No
Test	COVID0516	Yes	Yes	0.601811945	0.3981881	No
Test	COVID0564	Yes	Yes	0.942398548	0.0576015	No
Test	COVID0450	Yes	Yes	0.885789573	0.1142104	No
Test	COVID0714	Yes	No	0.888814926	0.1111851	No
Test	COVID0408	Yes	Yes	0.700852036	0.299148	No
Test	COVID0558	Yes	Yes	0.056852765	0.9431472	Yes
Test	COVID0540	Yes	Yes	0.26985541	0.7301446	Yes
Test	COVID0444	Yes	Yes	0.012335699	0.9876643	Yes
Test	COVID0456	Yes	Yes	0.34420839	0.6557916	Yes
Test	COVID0468	Yes	Yes	0.26985541	0.7301446	Yes
Test	COVID0498	Yes	Yes	0.045760725	0.9542393	Yes
Test	COVID0576	Yes	Yes	0.057154838	0.9428452	Yes
Test	COVID0504	Yes	Yes	0.006351133	0.9936489	Yes
Test	COVID0600	Yes	No	0.106978044	0.893022	Yes
Test	COVID0672	Yes	No	0.08792568	0.9120743	Yes
Test	COVID0588	Yes	No	0.028880829	0.9711192	Yes
Test	COVID0654	Yes	No	0.029438535	0.9705615	Yes
Test	COVID0666	Yes	No	0.124919437	0.8750806	Yes
Test	COVID0726	Yes	No	0.198130682	0.8018693	Yes
Test	COVID0474	Yes	Yes	0.077650517	0.9223495	Yes
Test	COVID0432	Yes	Yes	0.145361423	0.8546386	Yes
Test	COVID0462	Yes	Yes	0.06204395	0.9379561	Yes
Test	COVID0510	Yes	Yes	0.248548523	0.7514515	Yes
Test	COVID0768	Yes	Yes	0.377659917	0.6223401	Yes

Test	COVID0427	Yes	Yes	0.349406302	0.6505937	Yes
------	-----------	-----	-----	-------------	-----------	-----

422 ^a Intensive Care Unit

423 Note: (*) these patients were called as high-risk an initially annotated clinically as mild-COVID
424 cases. They subsequently died in the hospital within 28 days of admission

425

426 **Supplemental Table 1 & 2. Annotations and clinical characteristics for**
427 **COVID-19 patient samples used in this study.** Individual characteristics and
428 clinical features for the 116 COVID-19 patient samples used in this study (78
429 Training Set & 38 Test Set). CV: cardiovascular; DR: Dominican Republic; PEC:
430 pre-existing condition; T2DM: Type 2 diabetes mellitus.

431

432 **Supplemental Table 3. Prognostic calls for high-risk with 6-marker**
433 **EpiSwitch classifier model.** Prognostic calls of average and high risk for the
434 78 patients against disclosed attributes of severity: ventilation and /or ICU
435 support.

436

437 **Discussion**

438 The COVID-19 pandemic will represent a major public health crisis for months
439 to come. As a corollary, there remains a pressing need for prognostic testing
440 that can give individuals a readout of likely disease severity if infected with
441 SARS-CoV2, despite the rigorous social measures put in place to slow the
442 spread of the disease and the recent availability of vaccination options. Despite
443 the development and approval of vaccines by Pfizer-BioNTech, Moderna,
444 Janssen, and AstraZeneca for use in the US and EU, there are still many
445 individuals that will not be vaccinated due to 1) lack of access 2) ineligibility or

446 3) a personal choice. The worldwide vaccine roll-out itself has faced difficulties.
447 Despite initial optimism, vaccination rates in the EU are low [26, 27]. In the US,
448 the vaccine rollout has also faced adoption challenges. Around one third of
449 military personnel and a similar percentage of healthcare workers have opted
450 against vaccination, citing a variety of factors in their decision [28, 29]. Even as
451 the vaccine is available in many parts of the U.S., several states including
452 Minnesota, Michigan, Maryland, and Oregon have seen spikes in average new
453 daily COVID-19 cases in the month of April 2021 [30]. Even in countries where
454 vaccination campaigns have gone well from the standpoint of adoption rates
455 such as Israel and the United Kingdom, severe complications due to COVID-
456 19 are still seen [31, 32]. The emergence of novel coronavirus variants that
457 render some vaccines less effective also threatens to prolong the pandemic.
458 Currently there are six main variants circulating in the U.S.: the B.1.1.7
459 originating in the U.K.; the B.1.351 from South Africa; the P.1. first detected in
460 Brazil; and the B.1.427 and B.1.429, both originating in California and the highly
461 infectious B.1.617.2 (Delta) variant originating in India [33–36]. Based on
462 decades of research on viral evolution, the emergence of other strains in the
463 future is likely [37, 38]. As SARS-CoV-2 variants can spread faster than the
464 original strain and some variants may be resistant to the neutralizing antibodies
465 produced by individuals after vaccination, the risk of a widespread disease
466 resurgence and the continued societal burdens of an extended pandemic are
467 real [39–41].

468

469 While many molecular tests have been developed to detect the presence of the
470 SARS-CoV-2 virus, a reduced to practice molecular test with high prognostic

471 accuracy for severe outcomes following a SARS-CoV-2 infection represents an
472 unmet healthcare need. Here we extended on a previously published study and
473 describe the validation of a blood-based biomarkers for the prediction of severe
474 symptoms of COVID-19 disease, which can place individuals in the intensive
475 care support [15]. We identified a set of six biomarkers associated with systemic
476 immune-genetic dysregulation, that when processed and measured by qPCR
477 on human blood samples provided an accurate predictive readout on likely
478 COVID-19 disease severity. While to the best of our knowledge, a comparable
479 assay has not yet been reported on, the performance of the *EpiSwitch* assay
480 meets the urgent need for many individuals to have *a priori* knowledge of likely
481 disease severity in the event they are infected with the SARS-CoV-2 virus.

482

483 Interestingly, we found a significant enrichment of predictive markers at the
484 SWAP70 gene locus. The SWAP70 locus encodes a B-cell specific ATP and
485 calcium binding protein that is recruited to the plasma membrane following B-
486 cell activation with subsequent translocation to the nucleus. SWAP70 has been
487 shown to mediate immunoglobulin isotype switching in B-cells following
488 activation of the B-cell antigen receptor complex [42, 43]. This finding is
489 consistent with the recent reports of ongoing isotype switching in patients who
490 are critically ill with COVID-19 and the association of differential
491 immunoglobulin M (IgM)/IgG/IgA epitope diversity in mild or severe COVID-19,
492 especially in patients who succumbed to SARS-CoV-2 infection [44]. We also
493 observed that genes involved in haemostasis and blood clotting were found in
494 the regions covered by the predictive marker panel. This is consistent with
495 clinical reports of severe COVID-19 patients presenting clinically with a

496 'microvascular injury syndrome' with an associated procoagulant state as well
497 as clinical reports of hypercoagulation in patients with severe COVID-19 [45,
498 46]. Interestingly, it remains to be investigated if the identified microvascular
499 markers may have potential functional relevance to prothrombotic vaccination
500 responses in individual patients. The involvement of B-cell activation and
501 haemostasis are both in line with a prevailing view that systemic inflammation
502 and the cardiovascular clinical manifestations it triggers, all lie at the root of the
503 clinical symptomology seen in severe COVID-19 cases [47–49].

504

505 Extension of the current study to a wider distribution and larger number of
506 individuals could help define the regional, racial, and epigenetic prevalence of
507 high-risk biomarkers in these populations. A longitudinal observational study
508 with collections before and after resolution of the acute and chronic phases of
509 COVID disease will provide further invaluable insights into the mechanisms and
510 the long-term stability of the identified systemic biomarker signature. Early
511 evidence indicates that blood samples collected from patients before the onset
512 of the COVID pandemic reveal high-risk profiles in some individuals. This would
513 suggest that the biomarker profiles identified in this study are not emerging in
514 response to COVID infection, but rather represent a pre-existing default state
515 on the spectrum of outcome susceptibility.

516

517 There are several immediate implications of the results reported here. The
518 availability of a simple blood-based assay that provides a readout of likely
519 disease course if infected with SARS-CoV-2 is especially helpful for the triage
520 of individuals who either 1) do not have access to COVID-19 vaccines (due to

521 underlying medical conditions, location, or age for example) or 2) choose to
522 forgo vaccination for other reasons. It has been well appreciated that the
523 heterogeneity seen in COVID-19 disease outcomes are largely defined by the
524 host response, rather than the virus or its variants [15]. The emergence of viral
525 variants that can render some current vaccination strategies less effective and
526 the unknown longer-term path of the virus may make information about
527 individual risk of developing severe disease valuable for those who may be at
528 risk of re-infection. For individuals at the early stage of a confirmed SARS-CoV-
529 2 infection, the assay described here could assist with patient triage in hospital
530 settings and assist in clinical decision making with a direct impact on clinical
531 outcomes. For the currently non-infected population, the assay could help
532 inform individuals on the potential for high-risk severe outcomes in the event of
533 an infection. This could enable a review of preventative lifestyle decisions on
534 vaccinations, guide appropriate social distancing measures, and inform return
535 to work planning. Advanced knowledge of likely disease severity can also aid
536 patients and their physicians in making preparatory medical planning decisions
537 where appropriate. Last, when applied in larger scale, population-wide settings;
538 knowledge of pooled individual risk profiles can help health systems make
539 informed decisions about staffing and infrastructure needs in the event of a
540 pandemic resurgence.

541

542 **Conclusions**

543 Here we report on the development and validation of a predictive blood-based
544 assay that can identify, with high accuracy, individuals who are at the highest
545 risk of developing severe complications in COVID-19 disease. The 3D genomic

546 biomarker panel described here can be used to evaluate personalized risk of
547 complications prior to exposure to the SARS-CoV-2 virus. The assay described
548 here can assist individuals and their physicians in making informed decisions
549 on lifestyle, social, and return to work activities as well as guiding medical
550 intervention decisions, where necessary.

551

552 **Declarations**

553 C.K., A.W., F.S., M.S., J.W. E.H. and A.A. are full-time employees at Oxford
554 BioDynamics plc and have no other competing financial interests.

555

556

557 **Author Contributions**

558 EH, AA conceived the study, MS, EH and AR assisted with *EpiSwitch*[®] array
559 design. WM, AB and ZL assisted with design of experiments. MS and AA
560 planned and reviewed experiments. CK, AW, FCS and EH analysed the data.
561 RP, AD, PB, BE, TL performed experiments. RV, AB, DP, PAR, JM helped with
562 interpretation of the data and writing of the manuscript. WW, CK, EH, and AA.
563 wrote and reviewed the manuscript.

564

565 **Acknowledgements**

566 The authors would like to thank members of OBD Reference Facility Morgan
567 Thacker, Louis James, Thomas Lavin, Catriona Williams, Matt Parnell, Aemilia
568 Katzinski, Pieter Koorts, Kalsoom Rana and Jayne Green for direct operational
569 support and taking part in processing of clinical samples, Olly Hunter for
570 assistance in data analysis. In addition, we acknowledge Boca Biolistics LLC.
571 and Reprocell USA Inc. for the timely provision of high-quality clinical blood

572 samples and clinical annotations, and Agilent Technologies, Inc. for supply of
573 *EpiSwitch*[®] designed CGH microarray slides.

574

575 **Competing interests**

576 The authors declare that they have no competing interests.

577

578 **Consent for publication**

579 Written informed consent for publication was obtained from all authors.

580

581 **Availability of data and materials**

582 The datasets used and/or analysed during the current study are available from
583 the corresponding author on reasonable request.

584

585

586 **Ethics approval and consent to participate**

587 All patients signed informed consent forms prior to providing blood samples. All
588 ethical guidelines were followed.

589

590 **Funding**

591 This work was funded by Oxford BioDynamics.

592

593

594

595

596

597

598

599

600

601

602 **References**

603

- 604 1. Cucinotta D, Vanelli M. WHO declares COVID-19 a pandemic. *Acta*
605 *Biomed.* 2020;91.
- 606 2. Wang Z, Tang K. Combating COVID-19: health equity matters. *Nat Med.*
607 2020;26:458.
- 608 3. Pfefferbaum B, North C. Mental Health and the Covid-19 Pandemic. *N Engl*
609 *J Med.* 2020;383:510–2.
- 610 4. FDA EUAs for Molecular COVID-19 Diagnostic Tests.
611 [https://www.fda.gov/medical-devices/coronavirus-disease-2019-covid-19-](https://www.fda.gov/medical-devices/coronavirus-disease-2019-covid-19-emergency-use-authorizations-medical-devices/in-vitro-diagnostics-euas-molecular-diagnostic-tests-sars-cov-2)
612 [emergency-use-authorizations-medical-devices/in-vitro-diagnostics-euas-](https://www.fda.gov/medical-devices/coronavirus-disease-2019-covid-19-emergency-use-authorizations-medical-devices/in-vitro-diagnostics-euas-molecular-diagnostic-tests-sars-cov-2)
613 [molecular-diagnostic-tests-sars-cov-2.](https://www.fda.gov/medical-devices/coronavirus-disease-2019-covid-19-emergency-use-authorizations-medical-devices/in-vitro-diagnostics-euas-molecular-diagnostic-tests-sars-cov-2)
- 614 5. FDA EUAs for Anitgen COVID-19 Diagnostic Tests.
615 [https://www.fda.gov/medical-devices/coronavirus-disease-2019-covid-19-](https://www.fda.gov/medical-devices/coronavirus-disease-2019-covid-19-emergency-use-authorizations-medical-devices/in-vitro-diagnostics-euas-antigen-diagnostic-tests-sars-cov-2)
616 [emergency-use-authorizations-medical-devices/in-vitro-diagnostics-euas-](https://www.fda.gov/medical-devices/coronavirus-disease-2019-covid-19-emergency-use-authorizations-medical-devices/in-vitro-diagnostics-euas-antigen-diagnostic-tests-sars-cov-2)
617 [antigen-diagnostic-tests-sars-cov-2.](https://www.fda.gov/medical-devices/coronavirus-disease-2019-covid-19-emergency-use-authorizations-medical-devices/in-vitro-diagnostics-euas-antigen-diagnostic-tests-sars-cov-2)
- 618 6. Roberts M, Driggs D, Thorpe M, Gilbey J, Yeung M. Common pitfalls and
619 recommendations for using machine learning to detect and prognosticate for
620 COVID-19 using chest radiographs and CT scans. *Nat Mach Intell.*
621 2021;3:199–217.
- 622 7. G G, Zangrillo A, A Z, Antonelli M. Baseline Characteristics and Outcomes
623 of 1591 Patients Infected With SARS-CoV-2 Admitted to ICUs of the
624 Lombardy Region, Italy. *JAMA - J Am Med Assoc.* 2020;323:1574–81.
- 625 8. Zangrillo A, Beretta L, Scandroglio A, G M. Characteristics, treatment,
626 outcomes and cause of death of invasively ventilated patients with COVID-19
627 ARDS in Milan, Italy. *Crit Care Resusc.* 2020;22:200–11.

- 628 9. Yang X, Yu Y, Xu J, Shu H, Xia J. Clinical course and outcomes of critically
629 ill patients with SARS-CoV-2 pneumonia in Wuhan, China: a single-centered,
630 retrospective, observational study. *Lancet Respir Med*. 2020;8:475–81.
- 631 10. WHO. COVID-19 Clinical Management, Living Guidance. 2021.
632 <https://www.who.int/publications/i/item/WHO-2019-nCoV-clinical-2021-1>.
- 633 11. Polack F, Thomas S, Kitchin N, Absalon J. Safety and Efficacy of the
634 BNT162b2 mRNA Covid-19 Vaccine. *N Engl J Med*. 2020;383:2603–15.
- 635 12. Baden L, Sahly H, Essink B, Kotloff K, Frey S. Efficacy and Safety of the
636 mRNA-1273 SARS-CoV-2 Vaccine. *N Engl J Med*. 2021;384:403–16.
- 637 13. Voysey M, Clemens S, Madhi S, Weckx L. Safety and efficacy of the
638 ChAdOx1 nCoV-19 vaccine (AZD1222) against SARS-CoV-2: an interim
639 analysis of four randomised controlled trials in Brazil, South Africa, and the
640 UK. *Lancet*. 2021;397:99–111.
- 641 14. Tapia M. University of Chile-COVID-19.
642 [https://www.uchile.cl/noticias/174186/resultados-primer-estudio-de-](https://www.uchile.cl/noticias/174186/resultados-primer-estudio-de)
643 [efectividad-de-las-vacunas-en-chile](https://www.uchile.cl/noticias/174186/resultados-primer-estudio-de). Accessed 6 Nov 2021.
- 644 15. Hunter E, Koutsothanasi C, Wilson A, Santos F, Salter M, Powell R, et al.
645 3D genomic capture of regulatory immuno-genetic profiles in COVID-19
646 patients for prognosis of severe COVID disease outcome. *bioRxiv*. 2021.
- 647 16. Yan H, Hunter E, Akoulitchev A, Park P, Winchester DJ, Moo-Young TA,
648 et al. Epigenetic chromatin conformation changes in peripheral blood can
649 detect thyroid cancer. *Surg (United States)*. 2019.
- 650 17. Hunter E, McCord R, Ramadass AS, Greene J, Westra JW, Akoulitchev
651 A, et al. Comparative molecular cell-of-origin classification of diffuse large B-
652 cell lymphoma based on liquid and tissue biopsies. *Transl Med Commun*.

653 2020;5.

654 18. Alshaker H, Mills R, Hunter E, Salter M, Ramadass A, Skinner BM, et al.

655 Chromatin conformation changes in peripheral blood can detect prostate

656 cancer and stratify disease risk groups. *J Transl Med.* 2021.

657 19. Carini C, Hunter E, Ramadass AS, Green J, Akoulitchev A, McInnes IB, et

658 al. Chromosome conformation signatures define predictive markers of

659 inadequate response to methotrexate in early rheumatoid arthritis. *J Transl*

660 *Med.* 2018.

661 20. Salter M, Corfield E, Ramadass A, Grand F, Green J, Westra J, et al.

662 Initial Identification of a Blood-Based Chromosome Conformation Signature

663 for Aiding in the Diagnosis of Amyotrophic Lateral Sclerosis. *EBioMedicine.*

664 2018.

665 21. Jakub JW, Grotz TE, Jordan P, Hunter E, Pittelkow M, Ramadass A, et al.

666 A pilot study of chromosomal aberrations and epigenetic changes in

667 peripheral blood samples to identify patients with melanoma. *Melanoma Res.*

668 2015;:1. doi:10.1097/CMR.000000000000182.

669 22. Shah P, Hunter E, Potluri S, Zhang S, Dezfouli M, Back J, et al.

670 Development and validation of baseline predictive biomarkers for response to

671 avelumab in second-line (2L) non-small cell lung cancer (NSCLC) using

672 EpiSwitchTM epigenetic profiling. *J Immunother Cancer.* 2019;7.

673 23. Tsourkas A, Behlke M, Xu Y, Bao G. Spectroscopic features of dual

674 fluorescence/luminescence resonance energy-transfer molecular beacons.

675 *Anal Chem.* 2003;75:3697–703.

676 24. Fabregat A, Sidiropoulos K, Viteri G, Forner O. Reactome pathway

677 analysis: a high-performance in-memory approach. *BMC Bioinformatics.*

- 678 2017;18:142.
- 679 25. Szklarczyk D, Morris JH, Cook H, Kuhn M, Wyder S, Simonovic M, et al.
680 The STRING database in 2017: Quality-controlled protein-protein association
681 networks, made broadly accessible. *Nucleic Acids Res.* 2017.
- 682 26. COVID-19 Vaccination in the EU. [https://graphics.reuters.com/HEALTH-](https://graphics.reuters.com/HEALTH-CORONAVIRUS/EU-VACCINES/qmypmrelyvr/)
683 [CORONAVIRUS/EU-VACCINES/qmypmrelyvr/](https://graphics.reuters.com/HEALTH-CORONAVIRUS/EU-VACCINES/qmypmrelyvr/).
- 684 27. European Centre for Disease Prevention and Control: EU Vaccination
685 Rates. [https://www.ecdc.europa.eu/en/publications-data/data-covid-19-](https://www.ecdc.europa.eu/en/publications-data/data-covid-19-vaccination-eu-eea)
686 [vaccination-eu-eea](https://www.ecdc.europa.eu/en/publications-data/data-covid-19-vaccination-eu-eea).
- 687 28. Full Committee Hearing: “Update on the Department of Defense’s
688 Evolving Roles and Mission in Response to the COVID-19 Pandemic.”
689 [https://armedservices.house.gov/2021/2/full-committee-hearing-update-on-](https://armedservices.house.gov/2021/2/full-committee-hearing-update-on-the-department-of-defense-s-evolving-roles-and-mission-in-response-to-the-covid-19-pandemic)
690 [the-department-of-defense-s-evolving-roles-and-mission-in-response-to-the-](https://armedservices.house.gov/2021/2/full-committee-hearing-update-on-the-department-of-defense-s-evolving-roles-and-mission-in-response-to-the-covid-19-pandemic)
691 [covid-19-pandemic](https://armedservices.house.gov/2021/2/full-committee-hearing-update-on-the-department-of-defense-s-evolving-roles-and-mission-in-response-to-the-covid-19-pandemic).
- 692 29. Shaw J, Stewart T, Anderson K, Hanley S. Assessment of US Healthcare
693 Personnel Attitudes Towards Coronavirus Disease 2019 (COVID-19)
694 Vaccination in a Large University Healthcare System. *Clin Infect Dis.*
695 2021;ciab054.
- 696 30. United States Centers for Disease Control and Prevention: COVID Data
697 Tracker. [https://covid.cdc.gov/covid-data-tracker/#compare-trends_](https://covid.cdc.gov/covid-data-tracker/#compare-trends_newcases)
[newcases](https://covid.cdc.gov/covid-data-tracker/#compare-trends_newcases).
- 698 31. Rinott E, Youngster I, Lewis Y. Reduction in COVID-19 Patients Requiring
699 Mechanical Ventilation Following Implementation of a National COVID-19
700 Vaccination Program — Israel, December 2020–February 2021. *MMWR Morb*
701 *Mortal Wkly Rep.* 2021;70:326–8.
- 702 32. Frampton D, Rampling T, Cross A, Bailley H, Heaney J, Byott M. Genomic

- 703 characteristics and clinical effect of the emergent SARS-CoV-2 B.1.1.7
704 lineage in London, UK: a whole-genome sequencing and hospital-based
705 cohort study. *Lancet*. 2021.
- 706 33. Luring A, Hodcroft E. Genetic Variants of SARS-CoV-2—What Do They
707 Mean? *JAMA - J Am Med Assoc*. 2021;325:529–31.
- 708 34. M M, Bassi J, De Marco A, Chen A, Walls A, Di Iulio J. SARS-CoV-2
709 immune evasion by variant B.1.427/B.1.429. *bioRxiv*. 2021.
- 710 35. Davies N, Abbott S, Barnard R, Jarvis C. Estimated transmissibility and
711 impact of SARS-CoV-2 lineage B.1.1.7 in England. *Science (80-)*. 2021;372.
- 712 36. Torjesen I. Covid-19: Delta variant is now UK's most dominant strain and
713 spreading through schools. *BMJ*. 2021;373.
- 714 37. Sanjuan R, Nebot M, Chirico N, Mansky L, Belshaw R. Viral Mutation
715 Rates. *Journal Virol*. 2010;84:9733–48.
- 716 38. Koonin E, Dolja V, Krupovic M. Origins and evolution of viruses of
717 eukaryotes: The ultimate modularity. *Virology*. 2015;479:2–25.
- 718 39. Ikegame S, Siddiquey M, Hung C, Haas G, Brambilla L. Qualitatively
719 distinct modes of Sputnik V vaccine-neutralization escape by SARS-CoV-2
720 Spike variants. *medRxiv*. 2021;:03.31.21254660.
- 721 40. Huang S, Wang S. SARS-CoV-2 Entry Related Viral and Host Genetic
722 Variations: Implications on COVID-19 Severity, Immune Escape, and
723 Infectivity. *Int J Mol Sci*. 2021;22:3060.
- 724 41. Groves D, Rowland-Jones S, Angyal A. The D614G mutations in the
725 SARS-CoV-2 spike protein: Implications for viral infectivity, disease severity
726 and vaccine design. *Biochem Biophys Res Commun*. 2021;538:104–7.
- 727 42. Masat L, Caldwell J, Armstrong R, Khoshevenian H. Association of

- 728 SWAP-70 with the B cell antigen receptor complex. Proc Natl Acad Sci.
729 2000;97:2180–4.
- 730 43. Borggrefe T, Wabl M, Akhmendov A, Jessberger R. A B-cell-specific DNA
731 recombination complex. J Biol Chem. 1998;273:17025–35.
- 732 44. Ravichandran S, Lee Y, Grubbs G, Coyle E. Longitudinal antibody
733 repertoire in “mild” versus “severe” COVID-19 patients reveals immune
734 markers associated with disease severity and resolution. Sci Adv. 2021;7.
- 735 45. Helms J, Tacquard C, Severac F, Leonard-Lorant I, Ohana M. High risk of
736 thrombosis in patients with severe SARS-CoV-2 infection: a multicenter
737 prospective cohort study. Intensive Care Med. 2020;46:1089–98.
- 738 46. Magro C, Mulvey J, Berlin D, Nuovo G. Complement associated
739 microvascular injury and thrombosis in the pathogenesis of severe COVID-19
740 infection: A report of five cases. Transl Res. 2020;220:1–13.
- 741 47. Ackermann M, Verleden SE, Kuehnel M, Haverich A, Welte T, Laenger F,
742 et al. Pulmonary Vascular Endothelialitis, Thrombosis, and Angiogenesis in
743 Covid-19. N Engl J Med. 2020.
- 744 48. Babapoor-Farrokhran S, Gill D, Walker J. Myocardial injury and COVID-
745 19: Possible mechanisms. Life Sci. 2020;July:117723.
- 746 49. Magadum A, Kishore R. Cardiovascular Manifestations of COVID-19
747 Infection. Cells. 2020;9:2508.
- 748

**Refine/Build
Model**

200 markers

(Hunter et. al. 2021)

**Training Cohort
(78 patients)**

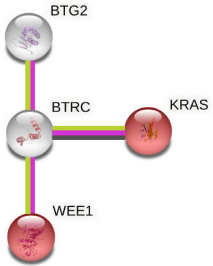
21 markers

6 markers

**Test
Model**

**Test Cohort
(38 patients)**





A

Test	Severe Outcome				Total
	Present	n	Absent	n	
Yes	True Positive	20	False Positive	2	22
No	False Negative	8	True Negative	8	16
Total		28		10	

Results

Statistic	Value	95% CI
Sensitivity	71.43%	51.33% to 86.78%
Specificity	80.00%	44.39% to 97.48%
Positive Likelihood Ratio	3.57	1.01 to 12.61
Negative Likelihood Ratio	0.36	0.18 to 0.69
Disease prevalence*	73.68%	56.90% to 86.60%
Positive Predictive Value*	90.91%	73.90% to 97.25%
Negative Predictive Value*	50.00%	34.02% to 65.98%
Accuracy*	73.68%	56.90% to 86.60%

B

Test	Severe Outcome				Total
	Present	n	Absent	n	
Yes	True Positive	66	False Positive	5	71
No	False Negative	9	True Negative	36	45
Total		75		41	

Results

Statistic	Value	95% CI
Sensitivity	88.00%	78.44% to 94.36%
Specificity	87.80%	73.80% to 95.92%
Positive Likelihood Ratio	7.22	3.16 to 16.48
Negative Likelihood Ratio	0.14	0.07 to 0.25
Disease prevalence*	64.66%	55.24% to 73.31%
Positive Predictive Value*	92.96%	85.25% to 96.79%
Negative Predictive Value*	80.00%	68.20% to 88.18%
Accuracy*	87.93%	80.58% to 93.24%